First-principles study of oxygen vacancies in $Mg_xZn_{1-x}O$ alloys

Adisak Boonchun and Walter R. L. Lambrecht
Department of Physics, Case Western Reserve University, Cleveland, Ohio 44106-7079, USA
(Received 13 May 2009; revised manuscript received 17 December 2009; published 13 January 2010)

A first-principles study of oxygen vacancies in $Mg_xZn_{1-x}O$ alloys is presented. Different types of oxygen vacancies are distinguished by their number of Mg and Zn nearest neighbors. The formation energy is found to be lowest for vacancies surrounded by four Zn nearest neighbors and is almost independent of the overall concentration in the alloy. Since this energy of formation enters the concentration via a Boltzmann factor, it implies that vacancies other than purely Zn surrounded are very unlikely even in relatively Mg-rich alloys. The defect energy level associated with the vacancy is a very deep donor level closer to the valence band than the conduction band. It does not follow the band gap with concentration but stays approximately fixed relative to the valence-band maximum. The defect level gradually increases with number of Mg neighbors.

DOI: 10.1103/PhysRevB.81.024103 PACS number(s): 61.72.jd, 71.55.Gs, 61.72.uj

I. INTRODUCTION

Zinc oxide (ZnO) is a wide-band-gap semiconductor with numerous applications. The band gap is 3.34 eV at room temperature. In order to make heterojunction devices such as light emitting devices and laser diodes, a material with a compatible material with higher band gap is required as barrier. $Mg_xZn_{1-x}O$ wurtzite alloys are the most widely used candidate alloys for this purpose in spite of the fact that MgO has the rocksalt structure. Kim *et al.*[1] reported that $Mg_xZn_{1-x}O$ is stable in the wurtzite structure for $x<0.375$. Above this concentration, the rocksalt structure becomes preferable. Ohtomo *et al.*[2–4] showed that it is possible to grow wurtzite structure of $Mg_xZn_{1-x}O$ alloy up to $x<0.33$. Given this interest in the $Mg_xZn_{1-x}O$ alloys it is also of interest to study how this will affect the defect physics of ZnO.

One of the most interesting and widely discussed defects in ZnO is the oxygen vacancy.[5–15] There has been a continuing dispute over this defect's energy levels. In particular, most calculations find this to be a negative-U center but the location of the $2+/0$ transition level is found to vary considerably depending on details of the computational method, such as the way in which gap corrections are applied, the size of supercell, the type of density functional, in particular, when allowing for hybrid functionals.

Considering this defect in the alloys, several new questions arise. We must now distinguish oxygen vacancies by their number of Mg atoms as nearest neighbor. We will label them as V_O^n for a vacancy with n Mg neighbors. Furthermore, the question arises how the different types of vacancy's electronic structure and energy of formation depend on the overall concentration of Mg in the alloy. Obviously, finding a vacancy surrounded by a large number of Mg is unlikely if the concentration is low. If the Mg atoms are placed randomly, the probability to find n Mg neighbors and $4-n$ Zn neighbors is $\binom{4}{n}x^n(1-x)^{4-n}$ in the alloy with x as Mg concentration. However, the difference in energy of formation of the different types of vacancies also comes into play in determining their relative abundance. As discussed previously by Bogusławski and Bernholc[16] for N vacancies in $Al_xGa_{1-x}N$ alloys, the probability the equilibrium concentration of vacancies of type n, is given by

$$[V_O^n] = \binom{4}{n} x^n (1-x)^{4-n} e^{-E_f/kT}. \quad (1)$$

In this study, we study the energies of formation of different types of vacancies and their defect energy levels. We show that the energy of formation increases strongly with the number of Mg neighbors, thus strongly favoring defects surrounded by all Zn atoms. The transition-energy levels of the latter are found to stay at constant energy relative to the valence band, even as the band gap of the alloy increases with Mg concentration. The V_O thus becomes deeper and deeper donors.

II. COMPUTATIONAL METHOD

We use the density-functional theory[17,18] in the local-spin-density approximation (LSDA) including Hubbard-U corrections, known as the LSDA+U method. The LSDA+U approach is commonly applied to the rather localized Zn-d states to incorporate their stronger Coulomb interaction. However, it is here also used to artificially shift up the Zn-s and Mg-s states which are the primary orbitals involved in the bottom of the conduction band. This is not really an intra-atomic effect but can nevertheless be treated as such because the conduction bands are mostly cation-s like and in the LSDA+U approach orbitals are shifted by $V_s=U_s(\frac{1}{2}-n_s)$, where n_s is the occupation number of this orbital. So, if $n_s=0$ the states are shifted up by $U_s/2$. The more ionic, the better this approach will work because then the antibonding conduction band is strongly cationlike and the corresponding bonding valence-band state is mostly purely anionlike, so n_s is indeed close to zero. This use of the LSDA+U approach was recently applied to the oxygen vacancy in ZnO by Paudel and Lambrecht.[12] We use $U_d=3.4$ eV and $U_s=43.54$ eV for Zn (Ref. 12) and $U_s=32.24$ eV for Mg so as to obtain the experimental Zn-d band position and values close to the experimental gaps of wurtzite ZnO and rocksalt MgO. The actual LDA+U potential applied is $|\phi_l\rangle V_l \langle\phi_l|$ with ϕ_l the l-partial wave inside the sphere at the linearized muffin-tin orbital (LMTO) linearization energy and thus the value of U_l required for a certain desired shift also depends crucially on the sphere radius. The values of U_s may seem

large but it should be remembered that these are not meant to be intra-atomic Coulomb energy values but rather chosen so that $U_s(\frac{1}{2}-n_s)$ represents the matrix elements of the self-energy operator at the conduction-band energy minus the LDA exchange correlation potential $\langle s|\Sigma(E_c)-v_{xc}^{\mathrm{LDA}}|s\rangle$. The LSDA+$U_d$+$U_s$ model is used to ensure correct band gaps but does not improve total energies of the bulk materials. Adding U_d has negligible effect on the lattice constant but adding U_s tends to increase it by 3%. To avoid errors from this inaccurate lattice constant, the calculations were all carried out at the LDA equilibrium lattice constant of the corresponding $Mg_xZn_{1-x}O$ alloy, which are all close to that of ZnO.[19]

The Kohn-Sham equations are solved using the full-potential LMTO method, developed by Methfessel *et al.*[20] A well-converged and optimized basis set is used with two sets of smoothing radii and Hankel function energies as envelope functions per angular-momentum channel up to $l=2$. For Brillouin zone integrations, a $2\times2\times2$ k-point mesh was found to give adequate convergence for the 36- and 54-atom supercells used.

The formation energy of a native defect D in charge state q is defined as

$$E_f(D^q) = E_{tot}(D^q) - E_{tot}(\mathrm{Mg}_x\mathrm{Zn}_{1-x}\mathrm{O}) + \mu_{\mathrm{O}} + q(E_{\mathrm{VBM}} + E_F), \tag{2}$$

where $E_{tot}(D^q)$ is the total energy of the supercell containing the defect in the charge state q, $E_{tot}(\mathrm{Mg}_x\mathrm{Zn}_{1-x}\mathrm{O})$ is the total energy of the $Mg_xZn_{1-x}O$ perfect crystal in the same supercell without the defect, E_{VBM} is the bulk valence-band maximum (VBM) energy with respect to the electrostatic potential average reference energy in the supercell and E_F is the Fermi energy measured from the VBM. By total energy we mean the energy minus the energy of the free atoms. μ_{O} is the chemical potential of oxygen which depends on whether the system is oxygen rich or cation rich. Under O-rich conditions, we assume equilibrium with O_2 molecules in the gas phase and ignoring the temperature-dependent rotational and translational free-energy contributions, we use half the binding energy of the oxygen molecule, $\mu_{\mathrm{O}}^g=-3.76$ eV as chemical potential.[21] In the cation-rich situation, we assume equilibrium with the $Mg_xZn_{1-x}O$ alloy and with the elemental metals Zn and Mg,

$$\mu_{\mathrm{O}} = \mu_{\mathrm{Mg}_x\mathrm{Zn}_{1-x}\mathrm{O}} - (1-x)\mu_{\mathrm{Zn}}^m - x\mu_{\mathrm{Mg}}^m$$

$$= \mu_{\mathrm{O}}^g + \Delta H_f(\mathrm{Mg}_x\mathrm{Zn}_{1-x}\mathrm{O}), \tag{3}$$

with $\Delta H_f(\mathrm{Mg}_x\mathrm{Zn}_{1-x}\mathrm{O})$ the energy of formation of the alloy from its elementary constituents. E_{VBM} in the defect containing supercell is determined by

$$E_{\mathrm{VBM}} = E_{\mathrm{VBM}}^b - V_l^b + V_l^{sc}, \tag{4}$$

where $E_{\mathrm{VBM}}^b - V_l^b$ is the position of the valence band in the perfect bulk crystal relative to some local potential reference, for example, the potential a the muffin-tin radius of one of the atoms. V_l^{sc} is the same reference level at the same type of atom chosen as far away from the defect as possible in the defect containing supercell. We thereby assume that on this atom the potential is already bulklike. We evaluate this term for the neutral defect only to avoid extra shifts from the long-range terms in the potential of the charged defect and further check it against the band structure of the supercell in which we can identify the defect gap states from the actual valence band. All energies are measured relative to the average electrostatic potential in the defect containing supercell.

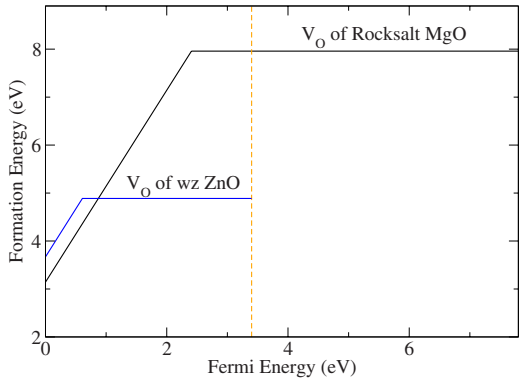

FIG. 1. (Color online) Calculated formation energies of oxygen vacancy in MgO and ZnO for the charge state with lowest energy of formation as function of Fermi level.

First, we determine the formation energy of the oxygen vacancy in the end compounds wurtzite ZnO and rocksalt MgO by a supercell approach using 36- and 54-atom supercells, which are a $3\times3\times1$ and $3\times3\times3$ repetition of the primitive unit cell, respectively. In order to calculate the formation energy of oxygen vacancies in $Mg_xZn_{1-x}O$ wurtzite alloys, the same supercell geometry with 36 atoms was used but with the Mg atoms placed randomly. A single Mg in a 36 atom cell, i.e., 18 cations, corresponds to about 5% Mg concentration. In this cell, we can pick the vacancy right next to the Mg or away from it, thus allowing us to study the V_{O}^0 and V_{O}^1 defects. Subsequently we replace one or more of the Zn neighbors of either the V_{O}^1 or V_{O}^0 by Mg, to construct models of the different types of V_{O}^n at different overall concentrations.

III. RESULTS

Figure 1 shows the calculated formation energy of the oxygen vacancy in wurtzite ZnO and rocksalt MgO (in oxygen-rich condition) as a function of Fermi energy E_F. The dashed vertical line indicates the calculated conduction-band minimum of wurtzite ZnO, which is 3.4 eV in our LSDA+U_d+U_s model, whereas the full range of the graph corresponds to the calculated band gap of rocksalt MgO. In p-type MgO, V_{O} is stable in the 2+ charge state and in n-type MgO, V_{O} is stable in the neutral charge state. In other words, we find it to be a negative-U system. The calculated $(2+/0)$ transition level of oxygen vacancy in rocksalt MgO is located at ~2.40 eV above the VBM. In a previous study by Janotti and Van de Walle,[22] a small range of stability is found for the 1+ charge state but the $(2+/+)$ and $(+/0)$ levels are found very close to each other and also near about 2.8 eV above the VBM. In wurtzite ZnO, we here find negative-U behavior with transition levels $(2+/0)$ at ~0.61 eV above

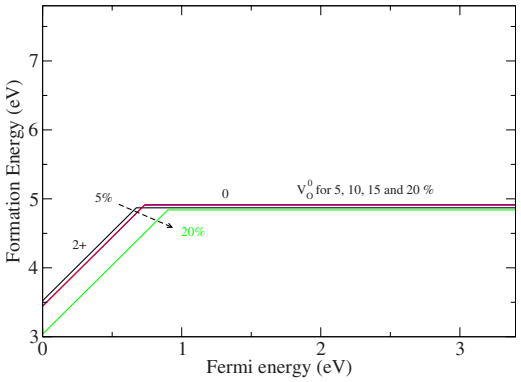

FIG. 2. (Color online) Calculated formation energies of various Mg concentration of oxygen vacancies V_O^0 in $Mg_xZn_{1-x}O$ wurtzite alloys. The black, blue, red, and green lines (from top to bottom) represent 5%, 10%, 15%, and 20% Mg concentration, respectively.

the valence-band maximum. As discussed by Paudel and Lambrecht[12] these levels are sensitive to the size of supercell. This level is about 0.80 eV in the same model in the extrapolation to infinite size given in Ref. 12. We can see that the energy where the neutral charge state becomes stable is significantly higher above the VBM in MgO (2.4 eV) than in ZnO (0.61 eV). We emphasize that our band structures on which these calculations are based already have the correct band gaps because of our LSDA+U_s+U_d approach, so no further *ad hoc* corrections are necessary.

Next, we consider oxygen vacancies in $Mg_xZn_{1-x}O$ wurtzite alloys. The calculated formation energies of V_O^0 in different alloy concentration x as function of Fermi-level position are shown in Fig. 2. All of these are obtained in the oxygen rich limit. We can see that the energy of formation of the neutral charge state is essentially independent of overall Mg concentration in the alloy. The charged states show a weak dependence on concentration. To illustrate this more clearly, the dependence of the $\epsilon(2+/0)$ transition levels for the V_O^0 are shown as function of alloy concentration x in Fig. 3. We can see that the defect level varies somewhat slower with concentration than the gap. This is consistent with the deep nature of the V_O donor level. Similar results apply to the other vacancy types with different number of Mg neighbors.

Having shown that the defect energies of formation for a given type of vacancy are only weakly dependent on the

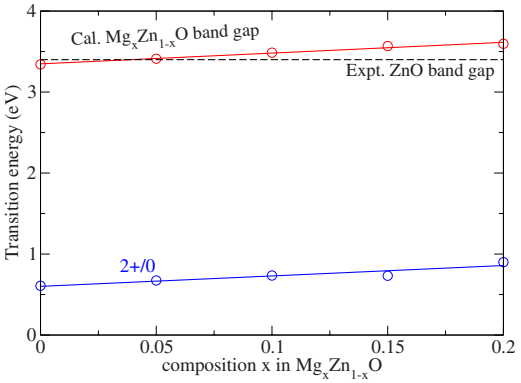

FIG. 3. (Color online) Transition-energy levels of the V_O^0 as function of alloy composition x in $Mg_xZn_{1-x}O$.

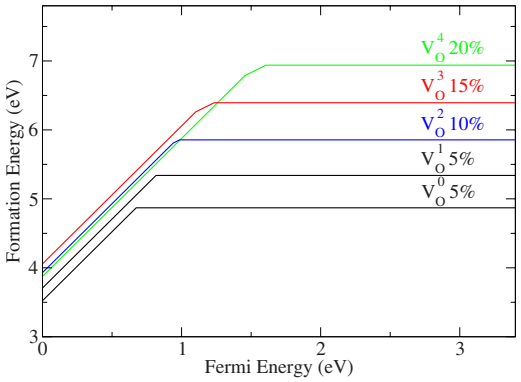

FIG. 4. (Color online) Calculated formation energies of various types of oxygen vacancies V_O^n with n Mg neighbors in $Mg_xZn_{1-x}O$ wurtzite alloys of different composition x. Again, black, blue, red, and green solid lines correspond to 5%, 10%, 15%, and 20% Mg concentration, respectively.

overall Mg concentration, we next examine the calculated formation energies for different vacancy types labeled by their number of Mg neighbors n as shown in Fig. 4. We can clearly see that the lowest energy of formation (in the neutral state) occurs for $n=0$ and the change for successively replacing each Zn by Mg as neighbor stays about constant and amounts to about 0.5 eV per Mg. We can also notice from this graph that the transition levels move gradually up with number of Mg neighbors. This is illustrated more clearly in Fig. 5. These results are also summarized in Table I. Although the energy of formation is only weakly dependent on overall concentration, we here give the actual concentration used for determining each type of vacancy.

We see that the energy of formation increases almost linearly with number of Mg neighbors. The implication of this is that defects with Mg as neighbors will be strongly suppressed. For example, the ratio of vacancies with one and zero Mg neighbors is given by

$$\frac{[V_O^1]}{[V_O^0]} = 4\left(\frac{x}{1-x}\right)e^{-E_f(1)+E_f(0)/kT}, \tag{5}$$

which for a typical growth temperature[2] of 900 K and $x=0.05$ is 8×10^{-5}. One can easily see that the random statis-

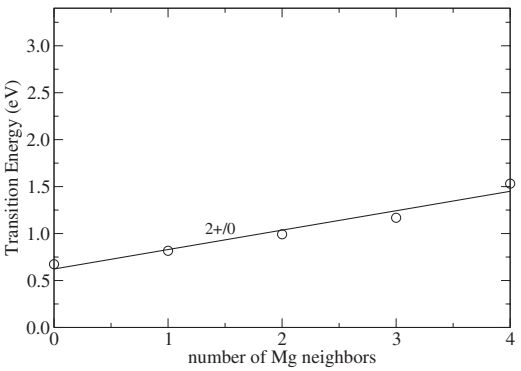

FIG. 5. Calculated transition energies for different vacancy types labeled by their number of Mg neighbors n.

TABLE I. Calculated transition levels for oxygen vacancy with different numbers of Mg atoms in $Mg_xZn_{1-x}O$ wurtzite alloys (in eV).

		Transition energy (eV)			Effective U
n	x	+/0	2+/0	2+/+	(eV)
0	0.05	0.66	0.67	0.68	−0.016
1	0.05	0.80	0.82	0.83	−0.025
2	0.10	0.99	0.96	0.93	0.046
3	0.15	1.23	1.17	1.10	0.132
4	0.20	1.67	1.53	1.46	0.151

tical prefactor is almost completely irrelevant compared to the factor depending on the energies of formation. Even in a 30% Mg alloy, the ratio is still of order 7×10^{-4}. Higher numbers of Mg neighbors in the vacancy are suppressed successively by similar factors.

From the results of Fig. 5 we can see that in cases of 10%, 15%, and 20% Mg concentration, we obtain positive-U behavior. Although this may, in part, be an artifact of the small supercell size, we can see that the value of $U=\epsilon(+/0)-\epsilon(2+/+)$ increases with the number of Mg neighbors as shown in Table I and Fig. 6. This indicates higher Coulomb energy cost for adding a second electron in the same defect level in defects with higher number of Mg neighbors. This is consistent with less electronic screening because of the larger band gap. The effective U not to be confused with the parameters U_d and U_s in our LSDA+U approach is mostly determined by the different degrees of relaxation in the different charge states. It is well known from the various previous studies of the oxygen vacancy in ZnO,[5–12] that in the neutral charge state, the four nearest neighbors move inward whereas for the double positive charge state the atoms move outward. In fact, this large change in relaxation, with a favorable rebounding in the neutral charge state is the origin of the negative-U behavior. We find that the four nearest-neighbors bond lengths move inward for V_O^0 and V_O^+ and moving outward for V_O^{2+} as shown in detail in Table II. However, we can see that the Mg-O bonds relax less inward than the Zn-O bonds. For example, for the V_O^1, we can see that compared to the bulk bond lengths, the Mg relaxes inward by 3% whereas the Zn neighbors relax inwards by 10%. Thus the more Mg atoms as neighbors, the less effective the relaxation in the neutral charge state. On the other hand, in the 2+ state, the outward relaxation of Mg is 13% and for Zn is 10%. This indicates a less favorable energy for the 2+ state for Mg atoms as neighbors. Both of these effects will tend to make the effective U more positive for vacancies with Mg as neighbors.

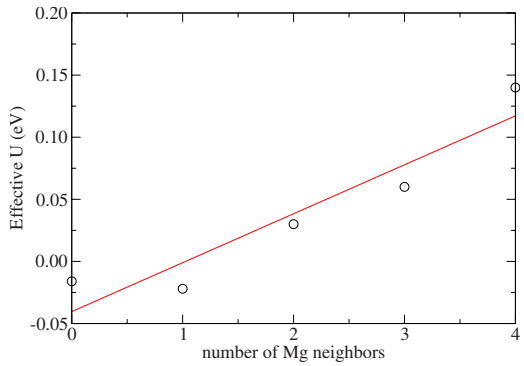

FIG. 6. (Color online) Calculated effective U energies increases with the number of Mg neighbors n.

The actual values of our transition levels depend sensitively on the approximations we have made here. First, there is our use of the LSDA+U_d+U_s functional. Although this functional gave results for ZnO in reasonable agreement with the B3LYP hybrid functional,[23,24] in terms the position of the 2+/0 transition level and the one-electron levels for the various charge states,[13] the more recent calculations using the HSE0 functional[25] by Oba *et al.*[11] place the 2+/0 transition level higher in the gap (at about 2.2 eV) and also did not give an unoccupied level in the gap for the 2+ state. Thus, although hybrid functionals are promising to overcome the band-gap problem, there is not yet a consensus on which hybrid functional is optimum for defect calculations.

Second, the finite-size corrections may be rather large for our small cell. The Coulomb image charge corrections can be written as[26,27]

$$E_{cor}=\frac{\alpha_M q^2}{\varepsilon L}+\frac{2\pi qQ}{3\varepsilon L^3} \tag{6}$$

with q the nominal charge of the defect, Q a quadrupole moment, L the linear size of the supercell, α_M a Madelung constant depending on the lattice, and ε the static dielectric constant of the semiconductor. As recently shown by Lany and Zunger[28] the quadrupole Q effectively behaves like qL^2 and thus can be incorporated in the first term by multiplying the latter by a factor which they found to be about 2/3. In practice we approximate the Madelung constant by writing it as $9/(10R)$ in terms of the equivalent Wigner-Seitz radius,[29,30] using atomic units. The dielectric constants for wurtzite $Mg_xZn_{1-x}O$ alloys have not yet been determined. The dielectric tensor components of bulk ZnO including vibrational contributions but not dipolar relaxation contributions[31] are $\varepsilon_\parallel=8.91$ and $\varepsilon_\perp=7.77$. Averaging this over the two directions and including a correction for the fact that LDA or GGA calculations overestimate the high-frequency part of the dielectric constants, a value of 9.5 was

TABLE II. The four nearest-neighbor bond lengths (in Å) around the oxygen vacancy in 0, 1+, and 2+ charge states.

		Bulk		Oxygen vacancy			
n	x	Site		Site	0	1+	2+
0	0	Zn-O	1.95	Zn-V_O	1.75	1.88	2.14
		Zn-O	1.95	Zn-V_O	1.75	1.88	2.14
		Zn-O	1.95	Zn-V_O	1.75	1.88	2.14
		Zn-O	1.96	Zn-V_O	1.75	1.79	1.90
0	0.05	Zn-O	1.95	Zn-V_O	1.76	1.89	2.15
		Zn-O	1.95	Zn-V_O	1.75	1.89	2.15
		Zn-O	1.95	Zn-V_O	1.75	1.89	2.13
		Zn-O	1.96	Zn-V_O	1.77	1.82	1.96
1	0.05	Mg-O	1.93	Mg-V_O	1.88	1.99	2.19
		Zn-O	1.95	Zn-V_O	1.76	1.89	2.15
		Zn-O	1.95	Zn-V_O	1.76	1.89	2.15
		Zn-O	1.96	Zn-V_O	1.77	1.82	1.95
2	0.10	Mg-O	1.94	Mg-V_O	1.87	2.03	2.27
		Mg-O	1.94	Mg-V_O	1.87	2.03	2.27
		Zn-O	1.96	Zn-V_O	1.76	1.90	2.17
		Zn-O	1.97	Zn-V_O	1.81	1.84	1.99
3	0.15	Mg-O	1.94	Mg-V_O	1.88	2.03	2.27
		Mg-O	1.94	Mg-V_O	1.89	2.04	2.28
		Mg-O	1.95	Zn-V_O	1.88	2.03	2.27
		Zn-O	1.97	Zn-V_O	1.81	1.82	2.00
4	0.20	Mg-O	1.95	Mg-V_O	1.89	2.04	2.33
		Mg-O	1.95	Mg-V_O	1.89	2.04	2.34
		Mg-O	1.95	Mg-V_O	1.89	2.04	2.33
		Mg-O	1.97	Mg-V_O	1.94	1.90	1.97

used by Oba *et al.*[11] for estimating the finite-size corrections. This is close to the static dielectric constant of rocksalt MgO of 9.83.[32] For simplicity, we thus use a constant value of about 9.5. This then leads to an upward shift of the single positive charge state by about 0.295 eV and of the double positive charge state by 1.18 eV, independent of Mg concentration or number of Mg neighbors to the defect since we used the same size cell in all cases. Including this correction would lower our $2+/0$ transition level by 0.59 eV to only 0.08 eV above the valence-band maximum and furthermore turn it into a positive-U center, with $2+/+$ at -0.205 eV and $+/0$ at 0.365 eV or $U_{eff}=0.57$ eV for the 5% Mg concentration and the vacancy with all Zn neighbors. While discussing finite-size effects here, we also comment on their effect in the work of Paudel and Lambrecht.[12] Adding the image charge correction to their result as done here, for their largest cell or 192 atoms, would give a value of 0.52 eV for $2+/+$, 0.71 eV for $+/0$, and 0.61 eV for $2+/0$ also leading to a positive-U defect and with values very close to those reported by Lany and Zunger[28] in their LSDA$+U_d+U_s$ model but not advocated by them as being the correct model for the vacancy. In the present case, our transition levels lie deeper to begin with even before image charge corrections are applied. It appears that other size effects, for example, due to the relaxation of the structure around the defect, or the close proximity of our defects along the z direction in our $3\times3\times1$ cell, leading to a direct bonding effect between the defect wave functions of neighboring defect may affect our present results. They do not follow the monotonic trend with supercell size seen in Paudel and Lambrecht's results.[12] Therefore adding the finite-size image charge corrections does not improve our results because other finite-size effect dominate.

We thus caution that our actual transition levels are strongly affected by finite-size effects. However, in spite of this uncertainty, it is clear that replacing Zn neighbors by Mg neighbors shifts the defect transition levels rather moderately. The defect level clearly shifts much less than the band gap. This is consistent with the fact that this defect level is deep in nature and does not follow the band gap like a shallow effective-mass state would. The trend of increasing effective U with number of Mg atoms, we believe can also be trusted in spite of the uncertainties on the starting value of the effective U for ZnO because it is based on the changes in atomic relaxation around the defect.

We also note that our main result on the energy of formation of the neutral defects which depends strongly on the number of Mg neighbors is independent of the image charge corrections. To further check this, we also performed a calculation for a larger (128 atom) cell containing one Mg out

of 64 cations or a concentration of about 1.5% Mg. We found the energies of the neutral oxygen vacancy for the Fermi level at the VBM to be 5.76 and 6.41 eV for the V_O^0 and V_O^1, respectively, showing that the latter has a 0.654 eV higher energy. This is even larger than we obtained in our small cells but confirms our main conclusion that such vacancies are very unlikely to form. Thus, our conclusion that vacancies with increasing numbers of Mg neighbors are strongly suppressed by the Boltzmann factor stays valid in spite of the finite-size errors.

All of the above results were obtained under oxygen-rich conditions, i.e., the least favorable for producing oxygen vacancies. The O chemical potential is then fixed and drops out of the comparison of the various defect-formation energies. When we consider O-poor conditions, the O chemical potential will depend on the oxygen concentration. Our values of the chemical potentials of Mg and Zn in their bulk metal states are, respectively, −2.44 and −1.75 eV as calculated in the LDA. In fact, it makes no sense to add the LSDA+U corrections here because the latter are material dependent and should be significantly smaller in the metallic screening environment. From Eq. (3) we can then see that μ_O varies with x in the same way as the energy of formation of the alloy. This dependence is shown in Fig. 7. This changing chemical potential in the oxygen-poor limit will now add a significant concentration dependence to the energy of formation of the defect, but it is essentially a linear dependence.

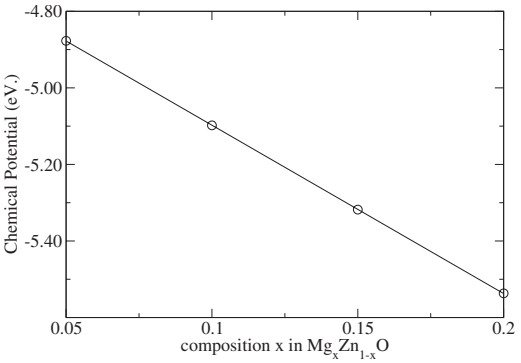

FIG. 7. Chemical potential of oxygen under O-poor conditions as function of alloy composition.

IV. CONCLUSIONS

The most important conclusion from our calculations is that the oxygen vacancy in $Mg_xZn_{1-x}O$ alloys prefers to be surrounded by Zn rather than Mg nearest neighbors. The energy cost per additional Mg is almost constant and about 0.5 eV in the neutral state of the defect. This energy cost is almost independent of the concentration. It implies that the concentration of defects with successively more Mg neighbors is strongly suppressed by a Boltzmann energy factor on top of the statistical prefactor which already suppresses it for concentrations $x<0.5$. This is important for alloys of practical consideration up to about $x=0.3$. Second, the oxygen vacancies stay deep donors as in pure ZnO. The transition levels do not vary significantly with concentration. There is a slight tendency of obtaining more positive-U values for the defects as more Mg's are added as nearest neighbor because of the less efficient relaxation of the latter in the neutral state. However, this is practically of no significance because these types of vacancies are strongly suppressed. Finally, in oxygen-poor conditions, there will be an additional concentration dependence arising from the varying oxygen chemical potential.

ACKNOWLEDGMENTS

We thank S. Limpijumnong for fruitful discussions. A.B. wishes to thank the Commission on Higher Education of Thailand for support.

[1] Y.-S. Kim, E.-C. Lee, and K. J. Chang, J. Korean Phys. Soc. **39**, s92 (2001).
[2] A. Ohtomo, M. Kawasaki, T. Koida, K. Masubuchi, H. Koinuma, Y. Sakurai, Y. Yoshida, T. Yasuda, and Y. Segawa, Appl. Phys. Lett. **72**, 2466 (1998).
[3] A. Ohtomo, M. Kawasaki, I. Ohkubo, H. Koinuma, T. Yasuda, and Y. Segawa, Appl. Phys. Lett. **75**, 980 (1999).
[4] A. Ohtomo, R. Shiroki, I. Ohkubo, H. Koinuma, and M. Kawasaki, Appl. Phys. Lett. **75**, 4088 (1999).
[5] S. B. Zhang, S.-H. Wei, and A. Zunger, Phys. Rev. B **63**, 075205 (2001).
[6] A. Janotti and C. G. Van de Walle, Appl. Phys. Lett. **87**, 122102 (2005).
[7] S. Lany and A. Zunger, Phys. Rev. B **72**, 035215 (2005).
[8] F. Oba, S. R. Nishitani, S. Isotani, H. Adachi, and I. Tanaka, J. Appl. Phys. **90**, 824 (2001).
[9] P. Erhart, A. Klein, and K. Albe, Phys. Rev. B **72**, 085213 (2005).
[10] P. Erhart, K. Albe, and A. Klein, Phys. Rev. B **73**, 205203 (2006).
[11] F. Oba, A. Togo, I. Tanaka, J. Paier, and G. Kresse, Phys. Rev. B **77**, 245202 (2008).
[12] T. R. Paudel and W. R. L. Lambrecht, Phys. Rev. B **77**, 205202 (2008).
[13] C. H. Patterson, Phys. Rev. B **74**, 144432 (2006).
[14] L. S. Vlasenko and G. D. Watkins, Phys. Rev. B **71**, 125210 (2005).
[15] S. M. Evans, N. C. Giles, L. E. Halliburton, and L. A. Kappers, J. Appl. Phys. **103**, 043710 (2008).
[16] P. Bogusławski and J. Bernholc, Phys. Rev. B **59**, 1567 (1999).
[17] P. Hohenberg and W. Kohn, Phys. Rev. **136**, B864 (1964).
[18] W. Kohn and L. J. Sham, Phys. Rev. **140**, A1133 (1965).
[19] A. Boonchun and W. R. L. Lambrecht, J. Vac. Sci. Technol. B **27**, 1717 (2009).
[20] M. Methfessel, M. van Schilfgaarde, and R. A. Casali, in *Electronic Structure and Physical Properties of Solids: The Use of the LMTO Method*, Lecture Notes in Physics Vol. 535, edited by H. Dreyssé (Springer-Verlag, Berlin, 2000), p. 114.

[21] R. O. Jones and O. Gunnarsson, Rev. Mod. Phys. **61**, 689 (1989).
[22] A. Janotti and C. G. Van de Walle, Nature Mater. **6**, 44 (2007).
[23] A. D. Becke, J. Chem. Phys. **98**, 5648 (1993).
[24] P. J. Stephens, F. J. Devlin, C. F. Chabolowski, and M. J. Frish, J. Phys. Chem. **98**, 11623 (1994).
[25] J. Heyd, G. E. Scuseria, and M. Ernzerhof, J. Chem. Phys. **118**, 8207 (2003).
[26] M. Leslie and M. J. Gillan, J. Phys. C **18**, 973 (1985).
[27] G. Makov and M. C. Payne, Phys. Rev. B **51**, 4014 (1995).
[28] S. Lany and A. Zunger, Phys. Rev. B **78**, 235104 (2008).
[29] P. Carloni, P. E. Blöchl, and M. Parinello, J. Phys. Chem. **99**, 1338 (1995).
[30] P. E. Blöchl, J. Chem. Phys. **103**, 7422 (1995).
[31] N. Ashkenov, B. N. Mbenkum, C. Bundesmann, V. Riede, M. Lorenz, D. Spemann, E. M. Kaidashev, A. Kasic, M. Schubert, M. Grundmann, G. Wagner, H. Neumann, V. Darakchieva, H. Arwin, and B. Monemar, J. Appl. Phys. **93**, 126 (2003).
[32] J. Fontanella, C. Andeen, and D. Schuele, J. Appl. Phys. **45**, 2852 (1974).